Nanostructure Deformation Behavior in Poly(ethylene terephthalate)/Polyethylene Drawn Blend As Revealed by Small-Angle Scattering of Synchrotron X-Radiation

9 AUTHORS, INCLUDING:

Stoyko Fakirov
University of Auckland
240 PUBLICATIONS **3,101** CITATIONS

SEE PROFILE

Anton Apostolov
Sophia University
54 PUBLICATIONS **1,027** CITATIONS

SEE PROFILE

Zlatan Zlatev Denchev
University of Minho
109 PUBLICATIONS **1,114** CITATIONS

SEE PROFILE

Nanostructure Deformation Behavior in Poly(ethylene terephthalate)/ Polyethylene Drawn Blend As Revealed by Small-Angle Scattering of Synchrotron X-Radiation

S. Fakirov,[†] O. Samokovliyski,[‡] N. Stribeck,*,[§] A. A. Apostolov,[†] Z. Denchev,[#] D. Sapoundjieva,[†] M. Evstatiev,[†] A. Meyer,[⊥] and M. Stamm[‡]

University of Sofia, Laboratory on Structure and Properties of Polymers, 1126 Sofia, Bulgaria; Institut für Polymerforschung, 01069 Dresden, Germany; Institut für Technische und Makromolekulare Chemie, Universität Hamburg, 20146 Hamburg, Germany; University of Minho, Department of Polymer Engineering, 4800-058 Guimarães, Portugal; and HASYLAB at DESY, 22603 Hamburg, Germany

ABSTRACT: The nanostructure deformation mechanism of a predrawn and annealed blend of poly-(ethylene terephthalate) (PET) and polyethylene (PE) (PET/PE: 50/50 by wt %) was studied. For the first time six-point small-angle X-ray scattering (SAXS) patterns were observed as a function of elongation in the investigation of a drawn polymer blend fiber sample. It was found that the meridional two-point pattern arises from PET and the inclined four-point one from PE. Long spacings and the angle between inclined reflections and fiber axis were determined as a function of draw ratio. At lower external strain (elongation up to 13%) the macrodeformation is related to conformational changes located only in amorphous material outside the lamellar stacks, whereas at higher elongation destruction of layer crystallites is observed, possibly due to pull-out of chains.

Introduction

SAXS is one of the few minimal invasive methods which can be used to study structural changes that take place on a nanometer scale during fiber spinning or stretching of semicrystalline or other multiphase polymer materials. Utilizing a synchrotron as the most powerful X-radiation source and a high-resolution 2D detector enables the recording of detailed scattering patterns with high accuracy during short exposure times.

The existence of unique six-point small-angle diffraction patterns has recently been reported in a systematic study on the deformation behavior of some oriented thermoplastic elastomers of poly(ether ester) (PEE) type[1−3] comprising poly(butylene terephthalate) (PBT) as hard domains and poly(ethylene glycol) (PEG) as soft domains. The peculiar pattern appears at a relative deformation ϵ of about 90%. At $\epsilon < 90\%$ two- and four-point patterns are registered. At higher deformations ($\epsilon = 100−200\%$) only two-point scattering diagrams are observed.[1−3]

The morphological interpretation of the six-point small-angle pattern from the earlier PEE studies[4,5] presumes the pull-out of interfibrillar tie molecules causing relaxation of the corresponding microfibrils. This notion is based on observations as a function of increasing elongation, showing that the long spacing of the two reflections on the meridian is decreasing considerably, while a four-point pattern is emerging, contracting toward the primary beam and, finally, vanishing. Within a particular deformation range ($\epsilon = $ 80−110%),[1] a clear six-point pattern was observed. The four-point subpattern indicates that, induced by the external strain, neighboring microfibrils connected by tie molecules align their hard domains with respect to each other, in this way basically forming a latticelike nanostructure.[1]

The present short communication reports on well-expressed six-point small-angle scattering diagrams obtained from a cold drawn blend of poly(ethylene terephthalate) (PET) and polyethylene (PE) studied at various deformations by means of synchrotron radiation.

The material under investigation is a precursor for the manufacturing of a recently developed nanostructured polymer−polymer composite in which an isotropic matrix is reinforced by microfibrils.[7,8] Such microfibrillar reinforced composites (MFC) are made from two immiscible polymers having different melting temperatures T_m^1 and T_m^2. After melt-blending, extrusion, and cold-drawing, a thermal treatment at temperatures between T_m^1 and T_m^2 turns the precursor into a MFC by isotropization of the low melting component.[8,9]

Experimental Section

Sample Description. Commercial engineering grade PET (Yambolen, Bulgaria) and PE (Burgas, Bulgaria) were dried in an oven at 100 °C for 24 h. Mixed in a ratio of 50/50 wt %, a PET/PE blend was prepared by extrusion in a Brabender single screw extruder (30 mm screw diameter; L/D ratio 25; 30−35 rpm; 2 mm capillary die). The extruder temperature zones were set at 210, 240, 260, 270, and 240 °C starting from the feed. The polymer strand was immediately quenched in water at 15−18 °C, moved through the bath by means of two rubber cylinders (60 mm diameter) rotating at a rate of 90 rpm.

The strands made were drawn in a tensile testing machine (Zwick 1464) at room temperature (strain rate 80 mm/min, draw ratio $\lambda = 3.6−4$), resulting in filaments of about 1 mm diameter. After drawing, stress recovery was induced by gently blowing the filaments with warm air (about 80 °C) for 1 min and finished by low-temperature annealing at 120 °C for 6 h with fixed ends in a vacuum.

[†] University of Sofia.
[‡] Institut für Polymerforschung, Dresden.
[§] Universität Hamburg.
[#] University of Minho.
[⊥] HASYLAB at DESY, Hamburg.
* To whom all correspondence should be addressed. E-mail: Norbert.Stribeck@desy.de.

Small-Angle X-ray Scattering Measurements. Synchrotron radiation generated at the beamline A2 of HASYLAB in Hamburg, Germany, was applied. The sample-to-detector distance was set to 1800 mm. A MFC reference sample was measured supplementary using a different machine setup, indicated by an increased central blind area. Two-dimensional (2D) small-angle X-ray scattering (SAXS) patterns were registered on image plates exposed between 2 and 5 min. An area of 900 × 900 pixels, each with a size of 176 μm × 176 μm, was read out and used for data evaluation. A stretching machine mounted in the pathway of the X-ray beam allowed for controlled elongation of the MFC precursor filaments in an ϵ range from 0 to 18.5%. Here and hereafter the elongation ϵ is defined as

$$\epsilon = 100(l - l_0)/l_0 \qquad (1)$$

with l_0 the initial and l the actual filament length, measured between marks placed close to the irradiated zone of the sample. After increasing the strain to the next step, a scattering pattern was recorded under stress. Then the polymer filament was released, the image plate was exchanged, and a pattern in the relaxed state was taken followed by a measurement under stress at higher deformation. The SAXS patterns are shown in Figure 1. For the reason of improved visual perception the images are "calibrated": Black level is intensity of the reflections on the meridian. The typical number of counts accumulated in the maxima of the reflections amounts to 20 000. The equatorial streak (void scattering) is overexposed in part.

Long spacings L were determined from both the two-point and from the four-point reflections. For that purpose straight sections were cut from the 2D scattering patterns along a radius (Figure 2). The resulting curves were fitted by Gaussian functions, and the L values were obtained from the positions of the fitted curve maximum. The intensity maxima of the four-point patterns are very close to the beam stop. Nevertheless, the maximum of the peaks is observed for all the samples except for the one with the elongation of $\epsilon = 18.5\%$. Only in that case we had to rely on the value from the fit without being able to cross-check the results visually with respect to the measured curve. Error bars reported in Table 1 are the asymptotic intervals of confidence computed from the parameter correlation matrix of the final step in the nonlinear regression. They are valid under the assumption that the Gaussian curve is a reasonable model for the peak shape.

Results and Discussion

Figure 1 presents SAXS patterns from predrawn ($\lambda = 3.8$) and annealed PET/PE blend material exposed under stress ($0 < \epsilon \leq 18.5\%$) and without external stress, respectively. The meridian or fiber axis (FA) is vertical in the gray scale images. Figure 1b is a 3D representation of the intensity map of Figure 1c. Figure 1h shows the scattering pattern of the MFC obtained by annealing the precursor at 180 °C for 4 h.

Apart from the MFC, well-expressed six-point SAXS patterns are observed in the whole deformation range irrespective of the presence or absence of external stress. The patterns obviously comprise a four-point pattern of "cloverleaf" or "butterfly" type, a two-point pattern on the meridian, and, finally, strong equatorial void scattering. The principal six-point character of the scattering diagram is best demonstrated in a 3D presentation (Figure 1b).

It is worth mentioning here that the first indication for SAXS six-point patterns was deduced from an evaluation of noisy scattering patterns recorded on PEE thermoplastic elastomers using a rotating anode source.[6] In following synchrotron radiation studies,[1−3] six-point patterns were confirmed for the elastomer material.
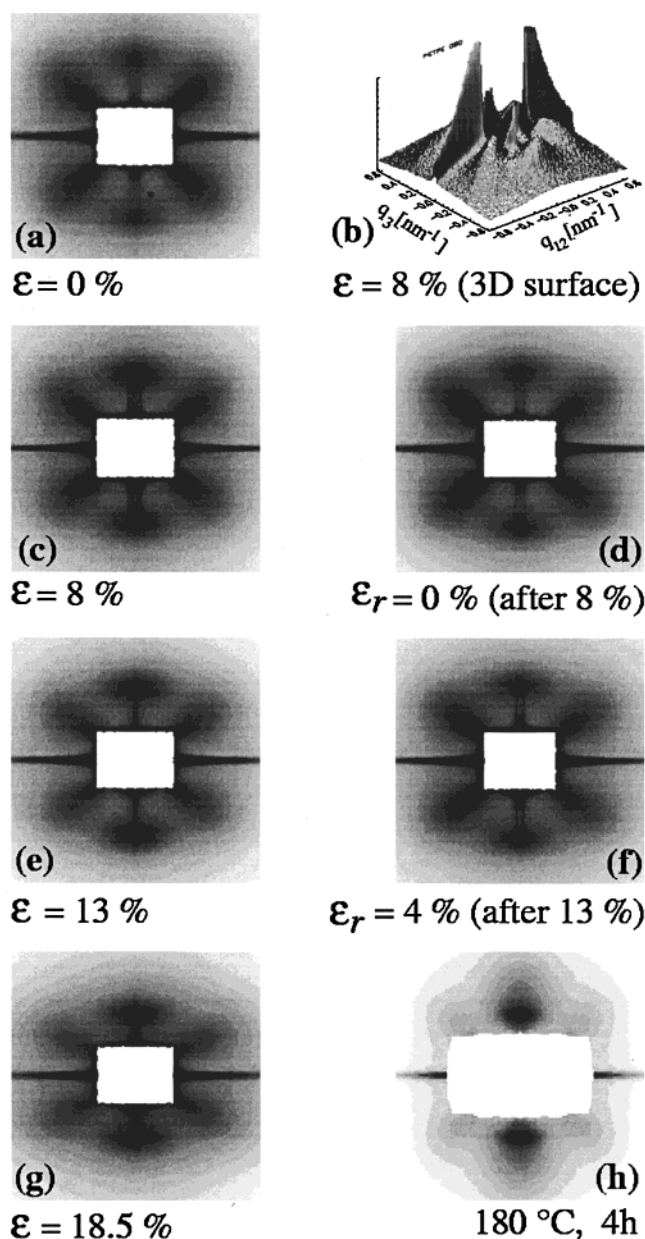

Figure 1. PET/PE 50/50 wt % blend predrawn ($\lambda = 3.8$) and annealed ($T_a = 120$ °C) ("MFC precursor"): 2D SAXS patterns (logarithmic gray scale) and a 3D representation taken under strain and without strain, respectively, as indicated by elongation ϵ or residual deformation ϵ_r, respectively. The fiber axis FA is vertical. In (b) it is parallel to the q_3-axis. The modulus of the scattering vector $q = (4\pi/\lambda) \sin \theta$ varies from -0.628 to 0.628 nm^{-1}. Pattern (h) originates from a sample measured at room temperature after converting the precursor into a MFC by heat treatment (180 °C, 4 h).

Concerning the nanostructure of the MFC precursor investigated here, what kind of information can be derived from the scattering patterns from Figure 1? Visual inspection of Figures 1a−g shows that the two semicrystalline components of the blend are highly oriented, similar to those MFC systems well characterized by wide-angle X-ray scattering (WAXS),[6] in which the basic morphological entities are microfibrils, as also was found by scanning electron microscopy.[9] The reflections on the meridian in Figure 1 give evidence for the presence of a nanostructure representing lamellar stacks perfectly oriented perpendicular to the stretching direction FA. The four off-meridian reflections can most probably be assigned to lamellar stacks being inclined
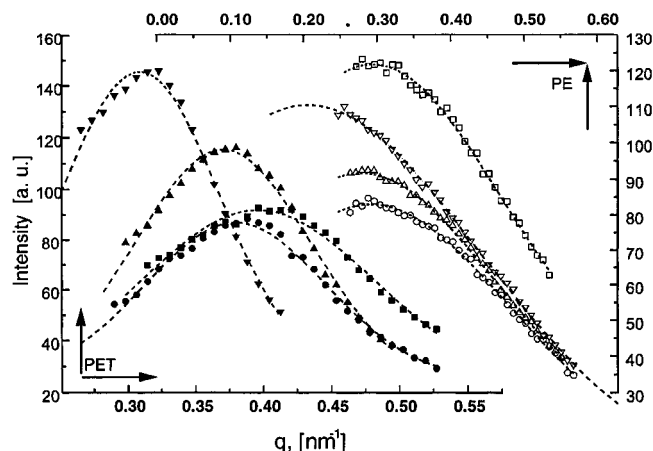
Figure 2. Radial direction intensity cuts (scattering intensity vs scattering vector q) from 2D scattering patterns for relative deformation ϵ in percent. For the PET reflections taken at the meridian (■, $\epsilon = 0\%$; ●, $\epsilon = 8\%$; ▲, $\epsilon = 13\%$; ▼, $\epsilon = 18.5\%$) and for PE inclined by ψ^{PE} (□, $\epsilon = 0\%$; ○, $\epsilon = 8\%$; △, $\epsilon = 13\%$; ▽, $\epsilon = 18.5\%$). Dashed lines show fits by Gaussian functions for every curve. Intensity is normalized with respect to primary beam intensity and irradiated volume.

Table 1. SAXS Pattern (cf. Figure 1) Evaluation Results from MFC Precursor PET/PE (50/50 wt %)[a]

total ϵ or residual deformation ϵ_r deformation (%)	L^{PET} (nm)	L^{PE} (nm)	ψ^{PE} (deg)
$\epsilon = 0.0$	15.87 ± 0.06	21.3 ± 0.5	52
$\epsilon = 8.0$	16.56 ± 0.05	21.4 ± 0.4	57
$\epsilon_r = 0.0$ (after 8.0, no stress)	16.00 ± 0.04	20.4 ± 0.3	53
$\epsilon = 13.0$	16.98 ± 0.04	22.4 ± 0.4	55
$\epsilon_r = 4.0$ (after 13.0, no stress)	15.58 ± 0.06	21.4 ± 0.4	54
$\epsilon = 18.5$	20.37 ± 0.08	30.2 ± 0.2	62

[a] Long spacing of PET (L^{PET}) and of PE (L^{PE}) as well as the inclination angle ψ^{PE} between the vertical axis and the direction of the inclined reflections.

with respect to FA, forming a second component. Obviously, each of both types of nanostructures are to be assigned to either the PET or the PE blend component.

In contrast to the case of drawn PEE, in which no void scattering was registered,[1-3] the blend shows a very strong equatorial scattering (Figure 1). This difference may partly be due to the fact that PEE is a block copolymer, i.e., a single component. The blend, in contrast, comprises two immiscible components. Because the equatorial scattering is almost constant as a function of deformation, one can assume that the equatorial streak originates from interfibrillar voids separating the components but not from interlamellar ones.

As described in the Experimental Section, semiquantitative evaluation of the patterns in Figure 1 yields numerical values for the long period L. The angle ψ between the inclined reflections and FA can be measured as well. It is equivalent to the angle between the lamellar stack normal direction and FA. Results are presented in Table 1.

Before discussing these results, let us answer the question of how to assign the two- and the four-point reflections to each of the blend components. Basically, this can be done by taking a SAXS pattern from the material at a temperature above T_m of PE. Another possibility is to convert the precursor material into a MFC by heat treatment and thereafter to check by a SAXS measurement at ambient temperature which reflections have been affected by the treatment. The first

approach causes extinction of the PE reflections, whereas the second results in transformation of the PE pattern into isotropic circles, if perfect isotropization is achieved. Figure 1h shows the SAXS pattern of the MFC made by annealing the precursor for 4 h at 180 °C. One observes that the intensity of the off-meridional peaks has decreased considerably, indicating partial isotropization of the corresponding component. Thus, the original four-point pattern made from the off-meridional peaks is assigned to the PE component.

Discussing the numerical data from Table 1, one can conclude that the long spacings, L^{PET} and L^{PE}, remain almost unaffected by smaller external deformation. Only at the last straining step before disruption of the sample ($\epsilon = 18.5\%$), both L^{PET} and L^{PE} increase. This may be explained by a process causing thin crystalline layers from the lamellar stacks to be destroyed by shear force. On the other hand, the invariable behavior of the long period during the preceding interval of straining indicates that no deformation takes place in the fraction of the material which is forming the lamellar stacks.

Studying the inclination angle ψ^{PE} of the PE lamellae as a function of elongation we observe an increase with the increase of ϵ (Table 1). This finding is to be expected taking into account that the stretching of the sample results in reduction of the fiber cross section while the fiber length is increased at the same time.

Considering the relative change of the scattering intensity of the two components (Figure 2), it is noticed that the PE peak intensity decreases by a factor of 2 during the first elongation step. Since shape and orientation of the peaks are hardly affected by deformation, relation to stack structure can be established without extensive evaluation effort. Such intensity decrease might be explained by the disappearance of 50% of the lamellar stacks in the sample, which should cause a more ductile flow of the whole material. However, a more reasonable explanation is founded on contrast variation. Even a moderate increase of the density in the amorphous layers and a corresponding decrease of the average density inside the polycrystalline lamellae would explain the finding. Concerning the PET reflections, similar reasoning would be arbitrary, because here the shape of the corresponding intensity profiles is strongly affected by deformation. Thus, it is inappropriate to discuss the apparent increase of peak intensity, because it goes along with a considerable contraction of the two-point pattern as a whole. From visual inspection only it thus appears impossible to estimate how the invariant of the PET component changes—a discussion irrelevant anyway, because of the obvious topological variations in the PET component as a function of deformation.

Conclusions

On the basis of the highly symmetric and extremely well-defined six-point SAXS patterns of the drawn PET/PE blend that were observed for the first time, one can follow the deformation behavior of the corresponding nanostructures. In the drawn and annealed PET/PE blend under investigation, the nanostructures of the two components from the blend respond independently to the external mechanical field. At lower external stress (ϵ up to 13%) the macrodeformation is related to conformational changes located only in amorphous material outside the lamellar stacks. At higher sample elongation ($\epsilon = 18.5\%$) destruction of crystallites takes

place, as was proved earlier for drawn PEE.[1−5] Similar to the earlier case, the reason for this destruction may be due to pull out of chains from the crystallites. More detailed study on the scattering behavior of this polymer blend is in progress, and the results will be reported in a subsequent paper.

References and Notes

(1) Stribeck, N.; Sapoundjieva, D.; Denchev, Z.; Apostolov, A. A.; Zachmann, H. G.; Stamm, M.; Fakirov, S. *Macromolecules* **1997**, *30*, 1329−1339.

(2) Stribeck, N.; Fakirov, S.; Sapoundjieva, D. HASYLAB Annual Report, 1998; pp 531−532.

(3) Stribeck, N.; Fakirov, S.; Sapoundjieva, D. *Macromolecules* **1999**, *32*, 3368−3378.

(4) Fakirov, S.; Fakirov, C.; Fischer, E. W.; Stamm, M. *Polymer* **1991**, *32*, 1173−1180.

(5) Fakirov, S.; Fakirov, C.; Fischer, E. W.; Stamm, M. *Polymer* **1992**, *33*, 3818−3827.

(6) Fakirov, S.; Denchev, Z.; Apostolov, A. A.; Stamm, M.; Fakirov, C. *Colloid Polym. Sci.* **1994**, *272*, 1363−1372.

(7) Evstatiev, M.; Fakirov, S. *Polymer* **1992**, *34*, 877−880.

(8) Fakirov, S.; Evstatiev, M. *Adv. Mater.* **1994**, *6*, 395−398.

(9) Evstatiev, M.; Fakirov, S.; Nikolov, N. *Polymer* **1996**, *37*, 4455−4463.

MA001317M